Lithos 376–377 (2020) 105800

Contents lists available at ScienceDirect

Lithos

journal homepage: www.elsevier.com/locate/lithos

Research Article

Contrasting platinum-group mineral assemblages of the Kondyor massif (Russia): Implications for the sources of HSE in zoned-type ultramafic massifs

Kreshimir N. Malitch [a,*], Igor S. Puchtel [b], Elena A. Belousova [c], Inna Y. Badanina [a]

[a] Zavaritsky Institute of Geology and Geochemistry, Ural Branch of the Russian Academy of Sciences, Vonsovsky str. 15, Ekaterinburg 620016, Russia
[b] Department of Geology, University of Maryland, College Park, MD 20742, USA
[c] Australian Research Council Centre of Excellence for Core to Crust Fluid Systems (CCFS) and GEMOC, Department of Earth and Planetary Sciences, Macquarie University, Sydney, NSW 2109, Australia

ARTICLE INFO

Article history:
Received 15 April 2020
Received in revised form 20 September 2020
Accepted 23 September 2020
Available online 25 September 2020

Keywords:
Kondyor massif
Pt–Fe alloys
Os–Ir alloys
Chromitite
Dunite
Clinopyroxenite
Re-Os-isotopes
Highly siderophile elements
Subcontinental lithospheric mantle

ABSTRACT

This study presents the first highly siderophile element (HSE: Re, Os, Ir, Ru, Rh, Pt, Pd, Au) abundance and Re–Os isotopic data for primary Pt–Fe minerals and Os-rich alloys from the Kondyor zoned-type ultramafic massif located in the southeastern part of the Siberian Craton, Russia. The Kondyor massif is composed of three zones: (A) the oldest dunite core with associated chromitites, with an age of emplacement of ~250 Ma, (B) a younger rim represented by metadunite, wehrlite, clinopyroxenite, and melanocratic gabbro that has transitional contacts with the dunite core, and (C) the youngest apatite-phlogopite-magnetite-rich clinopyroxenite stockwork exposed in the southwestern part of the massif. It has intrusive contacts with the dunite core and formed at ~125 Ma. Chromitites from zone (A) and clinopyroxenites from zone (C) analyzed in this study are characterized by distinct platinum-group mineral (PGM) assemblages dominated by Pt–Fe alloys in the former and cooperite with sperrylite and Pt–Fe alloys in the latter, with subordinate amounts of Os–Ir alloys present in both assemblages. The Re–Os isotope results identify a narrow range of initial $^{187}Os/^{188}Os$ values for Os–Ir alloys from the zone A chromitites (0.1249–0.1254) and the chromitites themselves (0.12466 ± 0.00005). Such chondritic initial $^{187}Os/^{188}Os$ values ($\gamma^{187}Os_{(T=250\ Ma)}$ ranging between −0.5 and + 0.1) indicate that the HSE budget of the chromitites and PGM from zone (A) was largely controlled by that of the mantle domain that evolved with long-term near-chondritic Re/Os, a notion that is also supported by the recent data of Luguet et al. (2019). In contrast, Os alloys from the zone C clinopyroxenites have initial $^{187}Os/^{188}Os$ values ranging between 0.1302 and 0.1308 (initial $\gamma^{187}Os_{(T=125\ Ma)} = +3.2$ to +3.7), indicative of a suprachondritic time-integrated Re/Os in the source of these rocks. The mineralogical and isotope-geochemical data point to a high-temperature origin of the studied PGM and at least two distinct sources of HSE in the ultramafic rocks of the Kondyor massif.

1. Introduction

A significant part of ultramafic zoned-type massifs (also termed the Uralian-type/Alaskan-type/Uralian-Alaskan-type and Aldan-type) is located in Russia (the Urals, Eastern Siberia, and the Far East). They are characterized by the presence of older dunitic cores and younger clinopyroxenitic rims and often closely spatially associated placer platinum deposits. The Kondyor massif is one of the several zoned clinopyroxenite-dunite complexes located within the Aldan Province, in the southeastern part of the Siberian Craton (Gurovitch et al., 1994; Malitch, 1999). It has attracted attention of researchers for more than half a century because of the spatially associated River Kondyor platinum placer deposit (Johan, 2002; Lazarenkov et al., 1992; Mochalov and Khoroshilova, 1998; Rozhkov et al., 1962; Sushkin, 1996, and references therein). According to the Amur Mining Company, about 100 metric tons of platinum have been mined from this deposit in the past 36 years.

The most common platinum-group minerals (PGM) that occur in this type of placer deposits are Pt–Fe alloys with subordinate Os–Ir alloys, although a great variety of other, less abundant, PGM have been also identified (Mochalov and Khoroshilova, 1998; Nekrasov et al., 1994; Shcheka et al., 2004). Among the alloys of the Pt-Fe-Ni-Cu system, isoferroplatinum and ferroan platinum are by far the most abundant, followed by tetraferroplatinum and tulameenite (Rudashevsky, 1989;

* Corresponding author.
E-mail addresses: dunite@yandex.ru (K.N. Malitch), ipuchtel@umd.edu (I.S. Puchtel), elena.belousova@mq.edu.au (E.A. Belousova), innabadanina@yandex.ru (I.Y. Badanina).

https://doi.org/10.1016/j.lithos.2020.105800
0024-4937/

Mochalov and Khoroshilova, 1998; Cabri and Laflamme, 1997; Malitch and Thalhammer, 2002; Evstigneeva, 2009; Malitch and Badanina, 2015; Kloprogge and Wood, 2018).

Despite numerous studies of zoned-type ultramafic massifs, the origin of these massifs and of the associated platinum mineralization remains unresolved (e.g., Augé et al., 2005; Garuti et al., 2002; Luguet et al., 2019; Malitch, 1999; Nekrasov et al., 1994; Okrugin, 2011; Pushkarev et al., 2015; Pushkaryov et al., 2002; Rudashevsky, 1989; Shukolyukov et al., 2012; Simonov et al., 2011; Tolstykh et al., 2005; Zaccarini et al., 2018; Zemlyanukhin and Prikhodko, 1997). The various models of origin of the mineralization proposed so far critically depend on accurate identification of the sources of the magmas and the timing of formation of the ore components. Since Re and Os are the highly siderophile elements (HSE: Re, Os, Ir, Ru, Rh, Pt, Pd, Au) with strongly contrasting partitioning behavior during mantle melting and magma differentiation, the Re–Os isotopic system is particularly useful (i) in distinguishing between crustal and mantle sources of the HSE due to the large fractionation of Re over Os between crust and mantle, and (ii) to calculate Re–Os model and Re-depletion ages (i.e., T_{MA} and T_{RD}, Shirey and Walker, 1998; Walker et al., 1989) of Ru–Os sulfides and Os–Ru–Ir alloys of mantle origin. An additional advantage of the Re–Os system when applied to studies of Os-bearing PGM is that these minerals contain osmium as a major element in their crystal structures, while being essentially devoid of Re. This feature permits accurate determination of the initial Os-isotope ratios, assuming that the Re–Os isotopic system in the PGM remained closed since the time of their formation and, therefore, reflects that of the source.

Only limited Os isotopic data for Os–Ir alloys and Ru–Os sulfides exist for different lithologies of zoned-type ultramafic complexes. Until recently, these have been restricted to four Os–Ir alloy grains in chromitites from the Kondyor massif (Malitch, 2004; Malitch and Thalhammer, 2002) and seven grains of laurite and Os–Ir alloys from chromitites of the Nizhny Tagil massif (Tessalina et al., 2015). Recently, Os isotopic data have been obtained also for 13 Pt–Fe alloy grains from a chromitite schlieren within the dunite core of the Kondyor massif (Luguet et al., 2019).

The Kondyor massif is mainly composed of three zones: (A) a dunite core with associated chromitites, (B) a metadunite (after Efimov, 1984), wehrlite, clinopyroxenite, and melanocratic gabbro rim, and (C) an apatite-phlogopite-magnetite-rich clinopyroxenite stockwork exposed in the southwestern part of the massif. To gain further insights into the genesis of platinum-group minerals, we have carried out a combined mineralogical, HSE abundance, and Re–Os isotope study of chromitites and PGM from the major rock types of the Kondyor massif. The samples studied were collected from: (1) chromitites within the dunite core (zone A), and (2) apatite-phlogopite-magnetite-rich clinopyroxenites (zone C). We integrated electron microprobe study of PGM and in-situ Re–Os LA-MC-ICP-MS analyses of Os–Ir alloys with whole-rock HSE abundance and Re–Os isotope analyses by ID N-TIMS and ID ICP-MS aiming at (i) evaluating the chemical compositions of Pt–Fe alloys from the different lithologies, and (ii) constraining the mantle vs. crustal origin of HSE/PGM from different lithologies within the Kondyor massif.

2. Geological background and samples

The Kondyor clinopyroxenite-dunite massif is located within the eastern part of the Aldan Shield in the Ayano-Maisky area, in the southeastern part of the Siberian craton (e.g., Gurovitch et al., 1994; Malitch, 1999; Nekrasov et al., 1994). The massif was emplaced into the Archean basement rocks (granitic gneisses, quartzites, and marbles) and the Late Proterozoic (Riphean) hornfelsed terrigenous-carbonaceous rocks of the Enninsk and Omninsk suites, forming a dome-like structure. Based on the gravimetric data, it is a vertical cylinder-shaped stock, extending down to a depth of ~10 km (Efimov and Tavrin, 1978). According to Lazarenkov and Landa (1992), Burg et al. (2009), and Guillou-Frottier et al. (2014), the Kondyor massif represents a solid-state mantle diapir of dunitic composition that was tectonically emplaced in the upper crust under near-solidus conditions. More recently, Luguet et al. (2019) proposed that the Kondyor massif represents the roots of an alkaline picritic volcano that constitutes remnants of an Early Triassic island arc.

In plane view on the surface, the Kondyor massif forms an oval body ~6 km in diameter and is mainly composed of dunite (olivine $Fo_{90–95}$), which forms the central core of the massif (Fig. 1). Lenticular bodies of chromitites up to 8 m in length and ~ 2 m thick are found in the dunite core, mainly in the southern, less eroded part, of the massif. Investigation of accessory PGM in the chromitites revealed the dominance of Pt–Fe alloys, with subordinate amounts of Os–Ir alloys, laurite (RuS_2), erlichmanite (OsS_2), hollingworthite (RhAsS), irarsite (IrAsS), platarsite (PtAsS), sperrylite ($PtAs_2$), tulameenite ($PtFe_{0.5}Cu_{0.5}$), hongshiite (PtCu), and geversite ($PtSb_2$) (Rudashevsky et al., 1992). This specific PGM assemblage is also found in the Quaternary sediments forming placer deposits that are closely spatially associated with the Kondyor massif (Mochalov and Khoroshilova, 1998; Shcheka et al., 2004). The HSE abundances and Re–Os isotopic compositions were obtained for PGM from veins of massive chromitites ~1 m thick that were traced in geological exploratory trenches for up to 4 m, with contacts dipping south at angles of 25-30° (sample K-17, Fig. 1), as well as from an irregular 40 × 5 × 3 cm schliere of massive chromitite with visible Pt–Fe minerals (sample K-2014, Figs. 1 and 2). Both chromitite samples were collected in the southern, less eroded part of the dunite core within the Kondyor massif.

The dunite core was intruded by vein-like, fine- to coarse-grained clinopyroxenites enriched in apatite, phlogopite, and magnetite, forming a stockwork-like zone C exposed in the southwestern part of the dunite core (Malitch, 1999, Fig. 1). The stockwork clinopyroxenites contain cooperite and sperrylite as dominant PGM, followed by subordinate Pt–Fe alloys, together with osmium (Os), tulameenite ($PtFe_{0.5}Cu_{0.5}$), sobolevskite (PdBi), braggite (Pt,Pd)S, keithconnite ($Pd_{20}Te_7$), irarsite (IrAsS), malanite ($CuPt_2S_4$), mertieite II ($Pd_8Sb_{2.5}As_{0.5}$), and a number of yet unnamed Pd-rich phases (Malitch, 1999; Rudashevsky et al., 1994). Sample K-11 is representative of this type of occurrence of Pt–Fe and Os alloys in the stockwork clinopyroxenite assemblage.

The dunite core (zone A) with associated chromitite lenses and veins are rimmed by metadunite (olivine $Fo_{78–88}$), wehrlite, clinopyroxenite, and melanocratic gabbro (zone B) up to 500 m in thickness, forming a concentrically zoned structure (Fig. 1). The metadunite and wehrlite

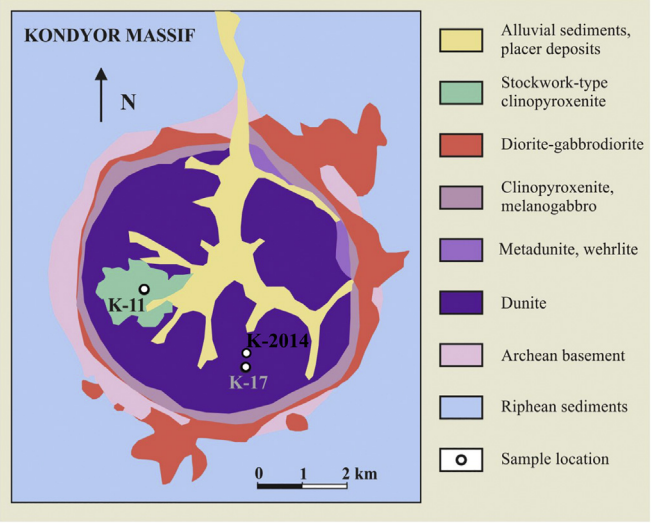

Fig. 1. Schematic geological map of the Kondyor clinopyroxenite-dunite massif (modified after Malitch, 1999).

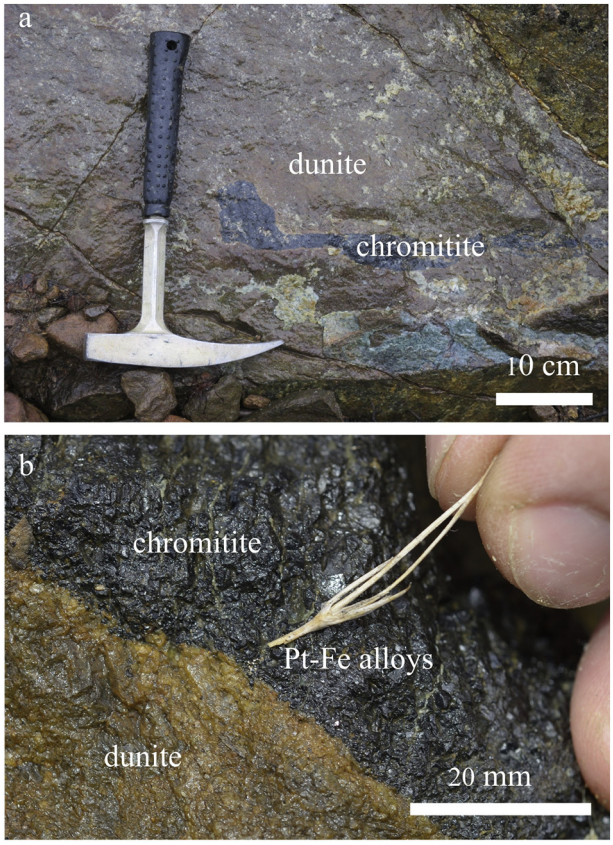

Fig. 2. Schliere of massive chromitite sample K-2014 with visible Pt–Fe minerals near the sharp contact with the dunite (a—Overview, b—Detail).

are thought to represent a reaction product between the zone A dunite and zone C clinopyroxenite. There is also a gradual transition from clinopyroxenites to melanocratic gabbro via plagioclase-bearing clinopyroxenite.

Minor veins and dykes that cut ultramafic rocks of the Kondyor massif are represented by leucocratic gabbro-plagioclasite and nepheline sienite pegmatite (Andreev, 1987; not shown in Fig. 1), whereas diorite and gabbrodiorite occur in the peripheral part of the massif (Fig. 1). These alkaline to subalkaline rocks form part of the post-Jurassic Aldan Complex (El'yanov and Andreev, 1991; El'yanov and Moralev, 1961).

3. Geochronological studies

The timing of formation of the Kondyor massif and its HSE mineralization remains controversial and continues to be the subject of debate. Some authors argued that the Kondyor massif was the result of polyphase intrusion of different magmas, with the ultramafic rocks formed in the Precambrian, and the intermediate, subalkaline and alkaline rocks originated in the Mesozoic (e.g., Efimov et al., 2012; El'yanov and Andreev, 1991; El'yanov and Moralev, 1961; Gurovitch et al., 1994; Malitch et al., 2012; Shnai and Kuranova, 1981). Others suggest that the entire intrusive suite is comagmatic and was formed in the Mesozoic (Orlova, 1992; Orlova et al., 1978).

Here, we used the most recent geochronological data to constrain the timing of formation of the two complexes (zones A and C) from which the samples of this study were collected and analyzed. A Rb–Sr and Sm–Nd isotope study of the clinopyroxenite zone C stockwork rocks yielded a mineral-whole-rock Rb–Sr isochron age of 126.7 ± 0.8 Ma and several mineral-whole-rock Sm–Nd isochron ages of between 131 ± 35 and 137 ± 26 Ma (Efimov et al., 2012). We used the combined Sm–Nd data for the whole-rock samples and mineral separates from the Efimov et al. (2012) study to calculate a combined Sm–Nd internal isochron age of 134 ± 18 Ma (initial $\varepsilon^{143}Nd = +6.3 \pm 0.1$) for the stockwork clinopyroxenite. These Rb–Sr and Sm–Nd isochron ages are consistent with the ^{190}Pt–^{4}He isochron ages obtained for Pt–Fe alloys from the stockwork apatite-phlogopite-magnetite clinopyroxenite assemblage (112 ± 7 Ma, Shukolyukov et al., 2012; 129 ± 6 Ma, Mochalov et al., 2016). These ages are interpreted to correspond to the time of intrusion of the clinopyroxenite assemblage (zone C rocks) into the dunite core (zone A rocks), and are coeval with the timing of the Mesozoic tectonomagmatic activity on the Aldan Shield (El'yanov and Andreev, 1991).

The recently obtained Pt–Os isotope data for Pt–Fe alloys from chromitites in the zone A dunites yielded an errochron (MSWD = 2,321,485) with an age of ~250 Ma (Luguet et al., 2019). These new data may imply that the Pt–Os system in the zone A dunites closed as early as 250 Ma in the asthenospheric mantle, likely at the time when they were injected in a near-solidus state in the upper crust as a mantle diapir (Burg et al., 2009). These data also likely imply that the dunite core (zone A) and the stockwork clinopyroxenite assemblage (zone C) rocks are genetically unrelated. The latter were likely the product of crystallization of invasive lamproitic melts that were progressively focused in the central part of the massif and drained into the vein conduits where they reacted with the wall-rock dunite to form the zone C stockwork assemblage (Burg et al., 2009).

Taking into account the above petrological, geochronological, and structural constraints, we adopt in this study the formation age of 250 Ma for the chromitites and associated PGM of the zone A dunite and 125 Ma as the age of formation of the zone C stockwork clinopyroxenite assemblage and associated PGM.

4. Analytical techniques

4.1. Mineral separation of PGM and electron microprobe analysis

To constrain the textural relationships of PGM with the associated silicate minerals, samples of chromitite and clinopyroxenite were first investigated in polished sections. Rock samples (1.0 kg each) were then disintegrated and milled, followed by sieving and removal of the fine fractions (<56 and 56–100 μm). The heavy minerals (including PGM) within these two fractions were concentrated by a hydroseparation technique (Malitch et al., 2001) at NATI Research JSC, St. Petersburg, Russia. This technique produced 1–4 mg of pure PGM material for each sample. Grains of minute PGM were investigated by scanning electron microscopy. Each heavy-mineral concentrate was then mounted in epoxy and the mounts were polished for further detailed microanalytical studies.

Electron microprobe analyses of PGM were carried out at the Montanuniversität Leoben (Austria), using an ARL-SEMQ microprobe with four wavelength-dispersive spectrometers (WDS) and equipped with a LINK energy dispersive analyser, and at the Institute of Geology and Geochemistry, UB RAS, Ekaterinburg, using a CAMECA SX-100 equipped with five WDS spectrometers and a Bruker energy dispersive spectrometer system. Quantitative WDS analyses were performed at 25 kV accelerating voltage and 20 nA sample current, with a beam diameter of ~1 μm. The following X-ray lines and standards have been used: RuLα, RhLα, PdLβ, OsMα, IrLα, PtLα, NiKα (all native element standards); FeKα, CuKα, SKα (all chalcopyrite); AsLα (sperrylite). Additional details of the analytical procedures used are described in Malitch et al. (2001) and Badanina et al. (2013b).

4.2. In situ analysis of Os isotopic compositions

In-situ Os-isotope analyses of Os–Ir alloys were carried out at the Geochemical Analysis Unit, CCFS/GEMOC laboratories, Macquarie University, Sydney, Australia, using analytical methods described in detail by Pearson et al. (2002) and González-Jimenéz et al. (2015). These analyses used a New Wave/Merchantek UP 213 laser ablation system

attached to a Nu Plasma Multicollector ICP-MS. Ablation was carried out with a frequency of 4 Hz, energies of 1–2 mJ/pulse and a spot size of 15 μm. A standard NiS bead (PGE-A) with 199 ppm Os (Lorand and Alard, 2001) and $^{187}Os/^{188}Os = 0.1064$ (Pearson et al., 2002) along with a natural Os alloy (i.e., $Os_{1.0}$) from the Guli massif (Merkle et al., 2012) were analyzed between PGM samples to monitor any drift in the Faraday cups. The isobaric interference of ^{187}Re on ^{187}Os was corrected for by measuring the ^{185}Re peak and using $^{187}Re/^{185}Re = 1.6742$. All the analyzed grains have very low Re contents ($^{185}Re/^{188}Os < 0.0005$), allowing for the isobaric interference of ^{187}Re on ^{187}Os to be accurately and precisely corrected for (Nowell et al., 2008). The Os isotopic data were reduced using the Nu Plasma time-resolved software, which allows the selection of the most stable intervals of the signal for integration. For Os–Ir alloys with grain sizes between 20 and 50 μm and Os contents between 30 and 98 wt%, a typical run duration of ~75 s was achieved with an average signal intensity of ~7.8 V on the Faraday cups. This gave an in-run precision on $^{187}Os/^{188}Os$ ranging from 0.04 to 0.2% relative (2SE). The external reproducibility of $^{187}Os/^{188}Os$ for the PGE-A standard during the period of measurements was 0.10652 ± 0.00013 (2SD; $n = 15$). Repeated analyses of a crystal of native osmium, which has been used to estimate the accuracy of the LA MC ICP-MS measurements, yielded $^{187}Os/^{188}Os = 0.12452 \pm 0.00004$ (2SD, $n = 27$). These data are consistent with two previous LA MC-ICPMS analyses via a New Wave COMPex-2 DUV 193 laser microprobe attached to Neptune MC ICP-MS, Russian Geological Institute, St. Petersburg for the same Os grain that gave a mean $^{187}Os/^{188}Os$ value of 0.12456 ± 0.00003 (2SD).

4.3. Analysis of HSE abundances and Os isotopic composition in whole-rock samples

Whole-rock HSE concentrations in the chromitite sample K-17 were determined at the Department of General and Analytical Chemistry, Montanuniversiät Leoben, through the application of the high pressure asher acid digestion and ID-ICP-MS method detailed by Meisel et al. (2001, 2003) and Paliulionyte et al. (2006). In brief, a test portion of 2 g of fine grained chromitite sample powder was spiked with a mixed enriched isotope HSE tracer, and digested in inverse aqua regia (5 ml of concentrated HNO_3 and 2 ml of concentrated HCl) at 300 °C and 125 bar for 10 h in a high pressure asher (HPA–S, Anton Paar, Graz, Austria). The osmium concentration was determined by sparging the OsO_4 that was formed during digestion into the ICP-QMS 7500ce. The remaining solution was dried down and the Ru, Rh, Pd, Re, Ir, and Pt concentrations were determined with an on-line separation procedure, as outlined by Meisel et al. (2003). Samples K-2014 and K-11 were analyzed for their HSE concentrations at the Analytical Centre of Institute Gipronickel (St. Petersburg) using Ni-fire assay followed by ICP-MS (mass spectrometer "iCAP-Qc" Thermo"), as detailed by Korotkov et al. (2016).

The Os-isotope composition and Os, Re, Ru, and Pd abundances of the chromitite sample K-2014 were determined at the Department of Geology, University of Maryland, following the analytical procedures detailed in Puchtel et al. (2016, 2018).

To obtain the Re–Os isotopic and HSE abundance data, ~100 mg of chromitite chips, 5 mL of purged, triple-distilled concentrated HNO_3, 4 mL triple-distilled concentrated HCl, and appropriate amounts of mixed ^{185}Re–^{190}Os and HSE (^{99}Ru,^{105}Pd,^{191}Ir,^{194}Pt) spikes were sealed in a chilled 25 mL Pyrex™ borosilicate Carius Tube and heated to 270 °C for 96 h. Osmium was extracted from the acid solution by CCl_4 solvent extraction (Cohen and Waters, 1996), back-extracted into HBr, and purified via microdistillation (Birck et al., 1997). Ruthenium, Pd, and Re were separated and purified using anion-exchange chromatography following a modified protocol of Rehkämper and Halliday (1997).

Osmium isotopic measurements were done via negative thermal ionization mass spectrometry (N-TIMS: Creaser et al., 1991). The sample was analyzed using a secondary electron multiplier (SEM) detector of a *ThermoFisher Triton* mass spectrometer at the *Isotope Geochemistry Laboratory (IGL)*, University of Maryland. The measured isotopic ratios were corrected for mass fractionation using $^{192}Os/^{188}Os = 3.083$. The in-run precision of measured $^{187}Os/^{188}Os$ was 0.04% relative. The $^{187}Os/^{188}Os$ ratio of 300–500 pg loads of the in-house *Johnson-Matthey* Os standard measured during the two-year period leading up to the current analytical session averaged 0.11376 ± 10 (2SD, $N = 64$). This value characterizes the external precision of the isotopic analyses (0.10%), which was used to estimate the true uncertainty on the measured $^{187}Os/^{188}Os$ ratio in the sample.

The measurements of Ru, Pd, and Re abundances were performed at the *Plasma Lab* of the Department of Geology, University of Maryland, on Faraday cups of a *ThermoFisher Neptune Plus* ICP-MS in static mode using 10^{13} Ohm amplifiers. Isotopic mass fractionation was monitored and corrected for by interspersing samples and standards. The external precision of the analyses was estimated on the basis of standard measurements performed during the period of the analytical campaign (Puchtel et al., 2020) to be $^{185}Re/^{187}Re = 0.25\%$, $^{99}Ru/^{101}Ru = 0.26\%$, and $^{105}Pd/^{106}Pd = 0.08\%$ relative (2SD). The accuracy of the data was assessed by comparing the results for the reference materials IAG MUH-1 (Austrian harzburgite), IAG OKUM (ultramafic komatiite), and NRC TDB-1 (Diabase PGE Rock Material) obtained at the *IGL* with the reference values (Supplementary Table A1). Concentrations of all HSE and Os isotopic compositions obtained at the *IGL* were within the uncertainties of the certified reference values.

The average TAB measured during the present analytical campaign was (in pg): Ru 6.0, Pd 17, Re 0.53, and Os 0.42 ($N = 9$). For the sample analyzed, the average TAB constituted less than 0.02% for Os, Ru, and Pd, and ~ 5.7% for Re of the total element analyzed. We therefore cite ±0.1% as the uncertainty on the concentrations of Os, Ru, and Pd and 5.7% as the uncertainty on the concentration of Re. The calculated uncertainty on the Re/Os ratio was propagated by multiplying the estimated uncertainties on the Re and Os abundances.

The initial $\gamma^{187}Os$ values were calculated as the per cent deviation of the isotopic composition at the time of the formation of the chromitite and the Os-rich alloys from the chromitite at 250 Ma, and the Os-rich alloys from the apatite-phlogopite-magnetite clinopyroxenite assemblage at 125 Ma, relative to the chondritic reference of Shirey and Walker (1998) at that time. The average chondritic Os isotopic composition at the time of the rock and Os-rich alloy formation was calculated using the ^{187}Re decay constant $\lambda = 1.666 \times 10^{-11}$ year^{-1}, an early Solar System initial $^{187}Os/^{188}Os = 0.09531$ at $T = 4558$ Ma, and $^{187}Re/^{188}Os = 0.40186$ (Shirey and Walker, 1998; Smoliar et al., 1996).

5. Results

5.1. PGM assemblages and compositional characteristics of Pt–Fe minerals and Os–Ir alloys

A list of all the PGM found in the samples studied is given in Table 1. Investigation of PGM grains from the zone A chromitites revealed a PGM assemblage dominated by Pt–Fe alloys with subordinate amounts of Os–Ir alloys (Os, (Os,Ir) and (Ir,Os)), laurite (RuS_2), erlichmanite (OsS_2), hollingworthite (RhAsS), irarsite (IrAsS), platarsite (PtAsS), sperrylite ($PtAs_2$), tulameenite ($PtFe_{0.5}Cu_{0.5}$), and some other PGM (Table 1). PGM assemblage from the zone C stockwork clinopyroxenites contain predominant cooperite and sperrylite, with subordinate Pt–Fe alloys, together with Os alloy, sobolevskite, braggite, keithconnite, irarsite, malanite, mertieite II, and a number of unnamed Pd-rich phases (Table 1).

Typical morphological features, characteristic textures of Pt–Fe alloy grains intergrown with Os–Ir alloys, laurite and irarsite are illustrated in Fig. 3. Os–Ir alloys were classified according to the nomenclature of Harris and Cabri (1991). Representative results of 92 electron microprobe WDS analyses of Pt–Fe alloys are presented in Table 2, those of Os–Ir alloys (from a total of 8 analyses) and several other PGM are shown in Table 1 and Fig. 4.

Table 1
Platinum-group mineral assemblages in rock lithologies from the Kondyor massif.

PGM in chromitite, samples K-17, K-2014	PGM in apatite-phlogopite-magnetite-bearing clinopyroxenite, sample K-11
Pt-Fe alloys	Cooperite (PtS)
Osmium (Os), (Os,Ir)	Sperrylite ($PtAs_2$)
Iridium (Ir,Os)	Pt-Fe alloys
Laurite (RuS_2)	Osmium (Os),
Erlichmanite (OsS_2)	Sobolevskite (PdBi)
Hollindworthite (RhAsS),	Braggite (Pt,Pd)S
Irarsite (IrAsS)	Keithconnite ($Pd_{20}Te_7$)
Platarsite (PtAsS)	Irarsite (IrAsS)
Malanite ($CuPt_2S_4$)	Malanite ($CuPt_2S_4$)
Cuproiridsite ($CuIr_2S_4$)	Mertieite II ($Pd_8Sb_{2.5}As_{0.5}$)
Cuprorhodsite ($CuRh_2S_4$)	Unnamed Pd-bearing PGM
Sperrylite ($PtAs_2$)	
Tulameenite ($PtFe_{0.5}Cu_{0.5}$)	
Geversite ($PtSb_2$)	
Unnamed PGE-BM sulfide	

Pt–Fe alloy grains from the zone A chromitite sample K-17 have sizes ranging from 10 to 1000 μm. They are mainly composed of primary Pt–Fe alloy, which revealed a rather constant composition corresponding to Pt_2Fe, whereas secondary tulameenite ($PtFe_{0.5}Cu_{0.5}$) is found in subordinate amounts (Figs. 3f and 4b). In the primary Pt–Fe alloy, Pt concentration ranges from 60.7 to 64.2 at.%, Ir from 0.40 to 3.48 at.%, Pd from 0 to 0.69 at.%, Rh from 0.82 to 2.55 at.%, and Os up to 0.24 at.% (Table 2, an. 1, 5, 7, 9, 11, 13, 15). The chemical compositions of the Os–Ir alloys range from osmium to iridium (Fig. 4a). Os–Ir alloys that were measured by LA-MC-ICPMS correspond to pure osmium (Table 2, an. 12, 14; Fig. 3h, i), Ir-rich osmium (Table 2, an. 10; Fig. 3g), and Os-rich iridium (Table 2, an. 16). These mineral compositions are typical of Os–Ir alloys that form inclusions in Pt–Fe alloy grains from zoned-type ultramafic massifs found in the Aldan Shield, e.g., Kondyor, Inagli, Chad (Malitch, 1999). Ru–Os sulfides have a narrow compositional range; Ru # [$100^{*}Ru_{at.\%}/(Ru + Os)_{at.\%}$] varies from 69 to 64, with high contents of Os (8.99–11.0 at. %), notable abundances of Rh (2.41–2.75 at. %), and moderate concentrations of Ir (0.76–1.36 at. %) (Table 2, an. 2–4; Fig. 3d). HSE sulpharsenides are represented by hollingworthite (RhAsS) – irarsite (IrAsS) solid solution series (Table 2, an. 6; Fig. 3e).

The Pt–Fe alloy grains from the zone C clinopyroxenite sample K-11 range in size from 65 to 300 μm. They show insignificant variations in composition, and correspond stoichiometrically to $(Pt,Pd,Rh)_{2.1}(Fe,Cu)_{0.9}$, with Pd ranging from 10.1 to 11.8 at.%, Rh 0.82 to 1.67 at.%, and Cu contents <3.81 at.% (Table 2, an. 13). The Pt–Fe alloy host tiny lamellae (up to 30 μm in the longest dimension) of nearly pure osmium (see Figs. 3i, 4a; Table 2, an. 14).

5.2. Whole-rock HSE concentrations

The total HSE concentrations in the chromitite sample K-17 from the zone A rocks analyzed in this study (Table 3) are 542 ppb, typical of those reported for the chromitites of the Kondyor massif (523 ppb:

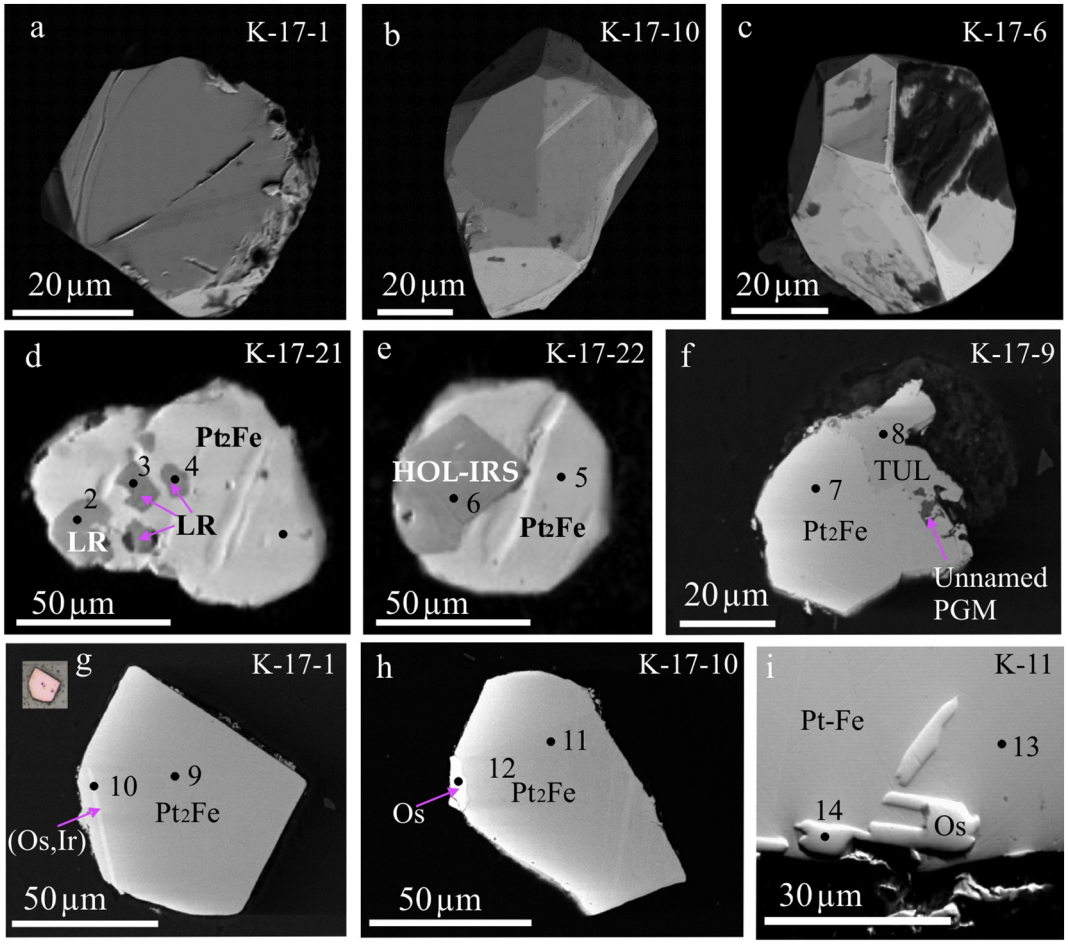

Fig. 3. Back-scattered SEM images of euhedral single and polyphase PGM grains from the chromitite sample K-17 (a–h) and clinopyroxenite sample K-11 (i) of the Kondyor massif taken before (a–c) and after (d–i) polishing. Numbers 1–14 denote areas of electron microprobe analyses corresponding to the same numbers in Table 2. Pt_2Fe—Ferroan platinum, LR—Laurite, HOL-IRS—Hollingworthite-irarsite series, TUL—Tulameenite, Unnamed PGM—(Pt,Rh,Fe,Cu)S, Os—Osmium.

Table 2
Electron microprobe (WDS) analyses of PGMs form the chromitite sample K-17 and clinopyroxenite sample K-11 from the Kondyor massif.

Analysis	1	2	3	4	5	6	7	8	9	10	11	12	13	14	15	16
Sample	K-17-21	K-17-21	K-17-21	K-17-21	K-17-22	K-17-22	K-17-19	K-17-19	K-17-1	K-17-1	K-17-10	K-17-10	K-11	K-11	K-17-6	K-17-6
Figure	3d	3d	3d	3d	3e	3e	3f	3f	3 g	3 g	3 h	3 h	3i	3i		
Mineral	Pt_2Fe	LR	LR	LR	Pt_2Fe	HOL-IRS	Pt_2Fe	TUL	Pt_2Fe	(Os,Ir)	Pt_2Fe	Os	Pt_2Fe	Os	Pt-Fe alloy	(Ir,Os)
Wt%																
Fe	10.84	0.00	0.00	0.00	10.92	0.00	11.17	13.40	11.27	0.00	10.87	0.00	11.02	0.00	11.05	0.00
Ni	0.37	0.00	0.00	0.00	0.26	0.00	0.91	1.83	0.42	0.00	0.60	0.00	0.12	0.00	0.50	0.00
Cu	1.81	0.00	0.00	0.00	1.38	0.00	1.70	8.98	1.38	0.00	1.57	0.00	1.72	0.00	1.04	0.00
Ru	0.00	31.74	29.79	29.91	0.00	2.68	0.00	0.00	1.80	4.29	0.00	2.21	0.17	0.00	0.00	3.97
Rh	1.43	4.39	3.81	3.79	0.77	21.98	1.43	0.57	0.00	0.63	1.63	0.45	0.60	0.80	1.36	2.71
Pd	0.00	0.00	0.00	0.00	0.00	0.00	0.47	0.49	0.42	0.00	0.36	0.00	7.65	0.00	0.50	0.00
Os	0.00	26.51	31.72	30.99	0.00	0.00	0.23	0.17	0.21	63.13	0.00	84.52	0.28	97.75	0.31	30.36
Ir	0.58	4.05	2.26	2.24	2.28	32.51	0.80	0.85	3.13	31.77	0.53	12.49	0.00	0.98	4.55	62.08
Pt	84.18	0.00	0.00	0.00	84.39	0.00	83.15	73.48	81.25	0.00	84.27	0.00	78.50	0.00	80.69	0.00
S	0.00	33.14	32.38	32.71	0.00	0.00	0.00	0.00	0.00	0.00	0.00	0.00	0.00	0.00	0.00	0.00
As	0.00	0.00	0.00	0.00	0.00	0.00	0.00	0.00	0.00	0.00	0.00	0.00	0.00	0.00	0.00	0.00
Total	99.21	99.83	99.96	99.64	100.00	57.17	99.86	99.77	99.88	99.82	99.83	99.67	100.06	99.53	100.00	99.12
At. %																
Fe	28.66	0.00	0.00	0.00	29.03	0.00	28.90	29.82	29.42	0.00	28.47	0.00	27.80	0.00	29.11	0.00
Ni	0.93	0.00	0.00	0.00	0.66	0.00	2.24	3.88	1.04	0.00	1.50	0.00	0.29	0.00	1.25	0.00
Cu	4.21	0.00	0.00	0.00	3.22	0.00	3.87	17.57	3.16	0.00	3.63	0.00	3.81	0.00	2.42	0.00
Ru	0.00	20.25	19.39	19.37	0.00	2.17	0.00	0.00	0.00	7.78	0.00	4.08	0.24	0.00	0.00	7.16
Rh	2.05	2.75	2.43	2.41	1.11	17.52	2.01	0.69	2.55	1.13	2.32	0.82	0.82	1.48	1.95	4.81
Pd	0.00	0.00	0.00	0.00	0.00	0.00	0.64	0.57	0.58	0.00	0.49	0.00	10.13	0.00	0.69	0.00
Os	0.00	8.99	10.97	10.67	0.00	0.00	0.17	0.11	0.16	60.81	0.00	82.97	0.21	97.55	0.24	29.12
Ir	0.45	1.36	0.77	0.76	1.76	13.87	0.60	0.55	2.37	30.28	0.40	12.13	0.00	0.97	3.48	58.91
Pt	63.70	0.00	0.00	0.00	64.22	0.00	61.57	46.81	60.72	0.00	63.19	0.00	56.70	0.00	60.86	0.00
S	0.00	66.65	66.44	66.79	0.00	34.69	0.00	0.00	0.00	0.00	0.00	0.00	0.00	0.00	0.00	0.00
As	0.00	0.00	0.00	0.00	0.00	31.75	0.00	0.00	0.00	0.00	0.00	0.00	0.00	0.00	0.00	0.00
Total	100.00	100.00	100.00	100.00	100.00	100.00	100.00	100.00	100.00	100.00	100.00	100.00	100.00	100.00	100.00	100.00
Ru #	–	69	64	64	–	–	–	–	–	–	–	–	–	–	–	–

Note. Analysis numbers 1–14 refer to points on Fig. 3; Pt_2Fe – ferroan platinum, LR – laurite, HOL-IRS – hollingworthite-irarsite series, Tul – tulameenite, (Os,Ir) – Ir-rich osmium, Os – native osmium, (Ir, Os) – Os-rich iridium; Ru number of laurite eqals to $100^{*}Ru_{at.\%}/(Ru + Os)_{at.\%}$.

Malitch, 1998). A total HSE content of 2157 ppm found in the chromitite sample K-2014 is quite uncommon and is due to an unusually high abundance of Pt–Fe alloy grains (ca. 80–100 grains with a size range from 5 to 1000 μm in diameter per polished block) revealed in this sample. Overall, the whole-rock HSE concentrations of the zone A chromitites have "M-shaped" BSE-normalized HSE patterns, with two peaks, at Ir and Pt, and with Pt enriched over Ir (Fig. 5; Table 3). The total HSE concentrations in the zone C clinopyroxenite sample K-11 (142 ppb) obtained in this study are almost identical to those reported for these rocks previously (Table 3, Malitch, 1998). This type of rock shows positively sloped HSE patterns (Fig. 5), with enrichment in Pt and Pd over other HSE and the Pt/Pd ratio varying from 1.1 to 1.4 (Table 3).

5.3. Whole-rock and in-situ mineral osmium isotope data

The Os isotopic data identified a narrow range of broadly similar initial $^{187}Os/^{188}Os$ values for the zone A chromitite samples (0.12466 ± 0.00005, $\gamma^{187}Os_{(T=250\ Ma)} = -0.55 \pm 0.04$, this study, Table 1, Supplementary Table A2 and 0.1257 ± 0.0001, $\gamma^{187}Os_{(T)} = +0.3 \pm 0.1$, Malitch et al., 2013).

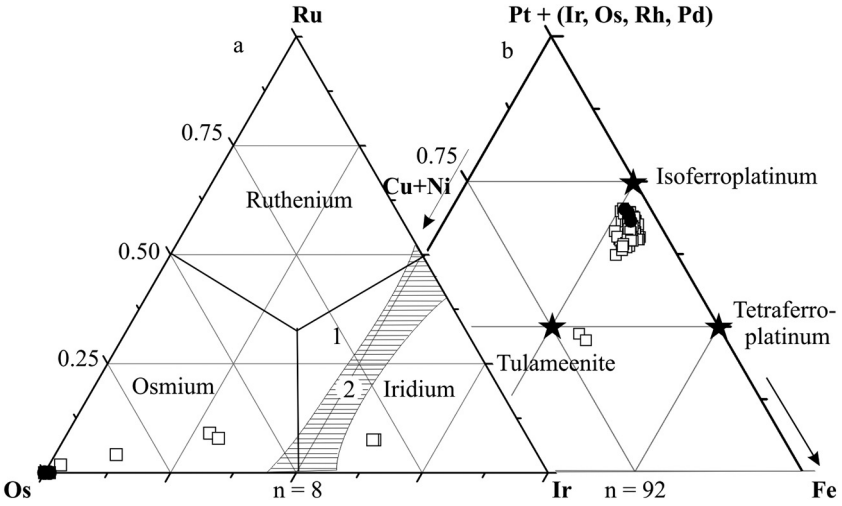

Fig. 4. Composition of Os—Ir alloys and Pt—Fe alloys in the ternary diagrams Ru – Os – Ir (a) and Pt + (Ir, Os, Ru, Rh, Pd) – Cu + Ni – Fe (b) from the chromitite sample K-17 (open squares) and the clinopyroxenite sample K-11 (solid circles) of the Kondyor massif. Fields 1 and 2—Ruthenoiridosmine and miscibility gap, respectively (after Harris and Cabri, 1991).

Table 3
Concentrations of highly siderophile elements (in ppb) and Os-isotopic composition of chromitite from the Kondyor massif.

Sample ID	Lithology	Os	Ir	Ru	Rh	Pt	Pd	Au	Re	ΣHSE	$^{187}Os/^{188}Os$	$\gamma^{187}Os_{(T)}$	Source
1	Chromitite	25 ± 16	52 ± 70	5 ± 4.2	12 ± 5.3	417 ± 58	12 ± 21	–	–	523	–		Malitch, 1998 (n = 12)
K-17	Chromitite	8	46	56	90	333	8.5	–	0.04	541.5			This study (University of Leoben)
K-2014	Chromitite	2780	14,700	2000	5200	2,099,000	28,000	550,000	–	2,701,680			This study (JSC Gipronickel, St. Petersburg)
K-2014 (2)	Chromitite	2227	–	543.1	–	–	8932	–	0.0886		0.12466 ± 0.00005	−0.55 ± 0.04	This study (University of Maryland)
2	Ap-Phl-Mgt Cpx	<5	<5	<3	6 ± 6	55 ± 92	49 ± 63	–	–	110	–	–	Malitch, 1998 (n = 20)
K-11	Ap-Phl-Mgt Cpx	<2	<3	<5	<5	77	54	11	–	142	–	–	This study (JSC Gipronickel, St. Petersburg)

Ap-Phl-Mgt Cpx – apatite-phlogopite-magnetite-rich clinopyroxenite. The initial $\gamma^{187}Os$ value ($\gamma^{187}Os_{(T)}$) was calculated as per cent deviation of the isotopic composition of chromitite at 250 Ma relative to the chondritic reference of (Shirey and Walker, 1998) at that time. The average chondritic Os isotopic composition at the time of the formation Os-rich alloys ($^{187}Os/^{188}Os(i)_{CH}$) was calculated using the ^{187}Re decay constant $\lambda = 1.666 \times 10^{-11}$ year^{-1}, an early Solar System initial $^{187}Os/^{188}Os = 0.09531$ at T = 4558 Ma, and $^{187}Re/^{188}Os = 0.40186$ (Shirey and Walker, 1998; Smoliar et al., 1996). Uncertainties are 2SE of the mean.

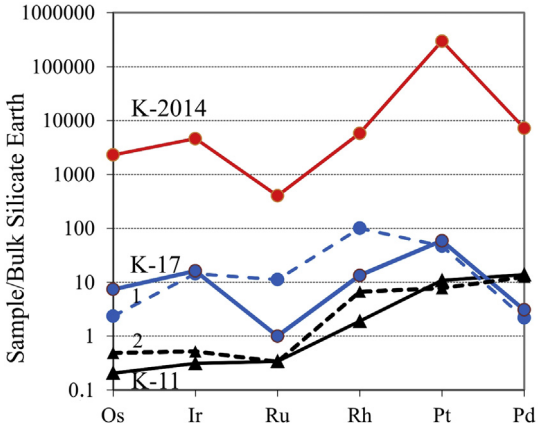

Fig. 5. BSE-normalized HSE patterns of the chromitite samples K-17, K-2014 and the clinopyroxenite sample K-11 from the Kondyor massif. Analyses 1 and 2 are those from Table 3. Normalizing values are from Becker et al. (2006).

The $^{187}Os/^{188}Os$ values for Os-rich alloys in association with Pt–Fe alloy grains from the zone A chromitites and zone C clinopyroxenites of the Kondyor massif are listed in Table 4. The Os-isotope data for four Os-rich alloy grains from the chromitites show a narrow range of $^{187}Os/^{188}Os$ values between 0.1249 and 0.1254, with a mean initial $^{187}Os/^{188}Os$ value of 0.1251 ± 0.0005 (2SE, n = 4) and the calculated average $\gamma^{187}Os_{(T=250\ Ma)} = -0.19 \pm 0.37$ (2SD, Supplementary Table A2). These new data are consistent with the earlier Os-isotope studies of Os-rich alloys from the Kondyor chromitite and placer deposits (Malitch, 2004; Malitch and Thalhammer, 2002), which gave a narrow range of $\gamma^{187}Os_{(T)}$ values from −0.4 to +0.1, indicating evolution of the mantle source of the zone A dunites and chromitites with a long-term chondritic Re/Os.

In contrast to the Os–Ir alloys from the zone A chromitites, the Os alloy from the zone C clinopyroxenite assemblage revealed much higher $^{187}Os/^{188}Os$ values ranging from 0.13022 ± 0.00004 to 0.13081 ± 0.00022 (Supplementary Table A2) and initial $\gamma^{187}Os$ ranging between +3.2 and + 3.7 (Table 4).

6. Discussion

6.1. PGM compositional constraints on distinct lithological sources

The HSE budget of the zone A chromitites is controlled by the PGM assemblage, where Pt–Fe alloys dominate over Os–Ir alloys, laurite and other PGM. The dominant role of Pt–Fe alloys in zoned ultramafic massifs is a distinct feature, particularly when compared with ophiolite-type massifs and stratiform complexes. This feature is expressed by "M"-shaped BSE-normalized HSE patterns (Fig. 5) (Malitch, 1998; Nixon et al., 1990; Zientek et al., 1992). Two maxima in the HSE distribution patterns (i.e., at Ir and at Pt, respectively) that characterize the zone A chromitites are clearly distinct from positively sloped BSE-normalized pattern of the zone C clinopyroxenites (Fig. 5), where HSE budget is controlled by Pt- and Pd-rich PGM.

Two varieties of Pt–Fe alloy grains were identified in the chromitite-bearing dunite core (zone A) of the Kondyor massif (Nekrasov et al., 1994): an early, high-temperature variety, typically with inclusions of Os–Ir alloys, Ru–Os sulfides, and Pt–Ir thiospinels in association with chromite (up to 64 wt% Cr_2O_3) and Mg-rich olivine Fo_{91-94}, and a late variety that occurs interstitially to chromite in lenses and veins of massive chromitite (up to 54 wt% Cr_2O_3) and almost lacks PGM inclusions. At Kondyor, where the depth of erosion of the dunite core is ~350–400 m, the range in Fe content of Pt–Fe alloys varies between

Table 4
Osmium isotope data for Os-rich alloys from the chromitite sample K-17 and clinopyroxenite sample K-11 from the Kondyor massif.

Sample, Figure	Atomic proportions	Os (V)	$^{187}Os/^{188}Os$	±2SE	$^{187}Re/^{188}Os$	±2SE	$^{187}Os/^{188}Os(i)$	$^{187}Os/^{188}Os(i)_{CH}$	$\gamma^{187}Os_{(T)}$
K-17-01, Fig. 3g	$Os_{61}Ir_{30}Ru_8Rh_1$	0.45	0.12487	0.00070	0.00070	0.00060	0.1249	0.12534	−0.38
K-17-06	$Ir_{59}Os_{29}Ru_7Rh_5$	5.29	0.12500	0.00030	0.00007	0.00010	0.1250	0.12534	−0.27
K-17-10-01, Fig. 3h	$Os_{83}Ir_{12}Ru_4Rh_1$	0.55	0.12514	0.00022	0.00020	0.00002	0.1251	0.12534	−0.16
K-17-10-02, Fig. 3h	$Os_{83}Ir_{12}Ru_4Rh_1$	2.82	0.12541	0.00048	0.00020	0.00002	0.1254	0.12534	0.05
K-11-1, Fig. 3i	$Os_{98.2}Rh_{1.3}Pt_{0.5}$	1.33	0.13022	0.00004	0.00001	0.00002	0.1302	0.12618	3.20
K-11-2, Fig. 3i	$Os_{98.2}Rh_{1.3}Pt_{0.5}$	1.18	0.13081	0.00022	0.00005	0.00016	0.1308	0.12618	3.67

The initial $\gamma^{187}Os$ value ($\gamma^{187}Os_{(T)}$) was calculated as per cent deviation of the isotopic composition for chromitite and Os-rich alloys from chromitite at 250 Ma and Os-rich alloys from apatite-phlogopite-magnetite clinopyroxenite at 125 Ma relative to the chondritic reference of Shirey and Walker (1998) at that time. The average chondritic Os isotopic composition at the time of the formation Os-rich alloys ($^{187}Os/^{188}Os(i)_{CH}$) was calculated using the ^{187}Re decay constant $\lambda = 1.666 \times 10^{-11}$ year^{-1}, an early Solar System initial $^{187}Os/^{188}Os = 0.09531$ at T = 4558 Ma, and $^{187}Re/^{188}Os = 0.40186$ (Shirey and Walker, 1998; Smoliar et al., 1996).

8.0 and 11.5 wt% (or between 22.6 and 33.1 at.% Fe), with the lowest and highest Fe values in the deepest and uppermost parts of the massif, respectively (Nekrasov et al., 1994). In addition, the early Pt–Fe alloys carry considerable amounts of other HSE impurities that also change with depth of crystallization. According to Nekrasov et al. (1994), in the least eroded areas of the dunite core, Pt–Fe alloy grains contain (wt%) 0.8–3.8 Ir, up to 2.9 Os, up to 1.5 Pd, and 0.5–1.8 Rh, whereas in the most deeply eroded zone of the dunite core, Pt–Fe alloys have (wt %) 2.5–5.3 Ir, 0.7–0.9 Os, 0.2–1.0 Pd, and 0.7–1.1 Rh, with intermediate PGE contents in Pt–Fe alloys in the other parts of the massif. In contrast, the late Pt–Fe alloys are almost free of other HSE, but retain the same Fe content with depth (Nekrasov et al., 1994). This is consistent with the observations of our study, which sampled chromitites (samples K-17 and K-2014, see Figs. 1, 6, and Table 2) from the least eroded southern part of the massif. The Pt–Fe alloy grains derived from the apatite-phlogopite-magnetite clinopyroxenite assemblage typically consist of cubic crystals locally coated with a film of Cu-bearing gold (Cabri and Laflamme, 1997). According to Nekrasov et al. (1994), the level of PGE impurities in the cubic crystals is generally low, similar to that in the late Pt–Fe alloys from the dunite core, and the Fe content is ~9.5–10.3 wt% (26.3–28.3 at.% Fe). According to Shcheka et al. (2004), Pt–Fe alloy grains commonly contain amphibole, calcic clinopyroxene, aegirine-augite, phlogopite, magnetite and apatite inclusions.

The Pt–Fe alloy grains from the apatite-phlogopite-magnetite clinopyroxenite in our study (sample K-11, Fig. 1) have comparable Fe contents (25.9–27.8 at.%), but unusually high contents of Pd (10.1–11.8 at.%, Fig. 6) and Rh (0.8–1.7 at.%), which can be attributed to the crystallization of notably fractionated melts, supported by a positively-sloping BSE-normalized HSE pattern of a host rock (Fig. 5). On the other hand, Pt–Fe alloy crystals, reported from the placer deposit at Kondyor (Fig. 11 in Cabri and Laflamme, 1997), might well be a reflection of growth in a late-stage flux-rich environment enriched in PPGE (i.e., Rh, Pt and Pd), as suggested by Barkov et al. (2017).

Variations in major and minor element abundances in Pt–Fe alloys from various geological settings and types of deposits, both lode and placer occurrences, have been evaluated by Barkov and Cabri (2019). These authors concluded that Pt–Fe minerals from placers, due to the similarity of their compositions, generally cannot be used as reliable tracers to identify their source rocks. By contrast, Pt–Fe alloys from the studied Kondyor rocks show systematic compositional differences (Table 2, Fig. 6). Pt–Fe alloys from the zone A chromitites have high contents of Ir (up to 3.1 wt%) and low contents of Pd (less than 0.50 wt%), whereas Pt–Fe alloys from the zone C clinopyroxenites are enriched in Pd (up to 7.7 wt%) and have moderate contents of Rh (up to 1.2 wt%). High Pd contents were also documented in Pt–Fe alloys from a clinopyroxenite of the Owendale zoned complex (Johan et al., 1989), as well as in Pt–Fe nuggets from alluvial placers in Madagascar with a proposed Alaskan-type source (Fig. 6; Augé and Legendre, 1992).

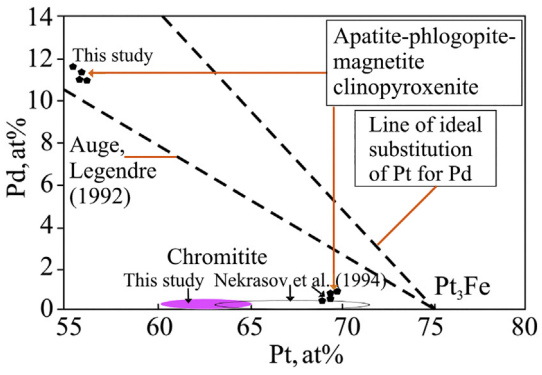

Fig. 6. Pt and Pd abundance data for Pt—Fe alloys from the chromitite and clinopyroxenite of the Kondyor massif.

Therefore, we propose that high contents of Ir or Pd in the Pt–Fe nuggets from the placer deposits at Kondyor may be considered a diagnostic feature of their host rock sources (i.e., chromitites versus clinopyroxenites).

6.2. Os-isotope constraints on the HSE sources and timing of PGM formation

According to experimental results and empirical data, Pt–Fe and Os–Ir alloys and laurite are considered to be formed during the very early stages of magmatic differentiation, under low fugacity of sulfur, and high-temperature conditions (e.g., Amossé et al., 2000; Andrews and Brenan, 2002; Badanina et al., 2013a; Brenan and Andrews, 2001; Fonseca et al., 2017; González-Jiménez et al., 2009; Johan et al., 1989). Early formation of Pt–Fe alloys with Os–Ir inclusions at high temperatures implies that the Os isotopic composition of Os–Ir alloys reflects that of the source region at the time of their formation.

The osmium isotope results identify a narrow range of initial $\gamma^{187}Os$ values for the Os–Ir alloys from the zone A chromitites (between −0.5 and + 0.1) that are identical, within uncertainty, to the initial $\gamma^{187}Os$ values of the Os-rich alloys from the chromitites and placer deposits (from −0.6 to −0.1: Malitch and Thalhammer, 2002; Malitch, 2004) and the bulk chromitite (initial $\gamma^{187}Os = -0.5$, this study, Fig. 7 and initial $\gamma^{187}Os = +0.3$: Malitch et al., 2013). The observed Os isotope similarity between PGM and the chromitite indicates that the osmium isotope budget of the chromitite was controlled by Os–Ir alloys and Pt–Fe minerals. A similar conclusion was reached during the earlier Os-isotope study of whole rocks and PGM from chromitite of the Nizhny Tagil zoned-type massif within the Uralian Platinum Belt (Tessalina et al., 2015). Much like the Kondyor, the Os isotopic compositions of Os–Ir alloy and laurite, measured by N-TIMS and LA MC-ICP-MS, respectively, were identical, within uncertainty, with that of the whole-rock, implying that the whole rock Os-isotope budget was largely controlled by laurite and Os–Ir alloy. Most likely, the ore-forming system, invariably related to the zone A dunites, was driven by mantle-derived fluids that mobilized and concentrated chromite and HSE in the upper parts of the dunite bodies during their ascent. This hypothesis could explain the fact that apical parts of the massifs are enriched in chromitites, representing the most important PGM source for platinum placer deposits. Our results are consistent with earlier findings (Malitch et al., 2002), where a narrow range of similar Os isotopic compositions was

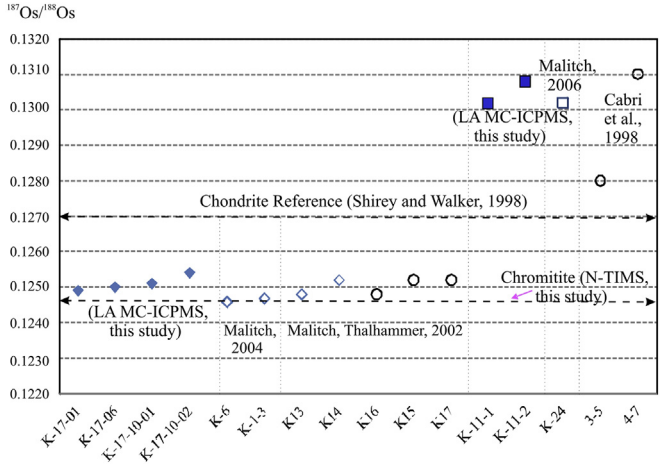

Fig. 7. Os isotopic composition of Os-rich alloys from the chromitite, clinopyroxenite, and placer deposits of the Kondyor massif. Data for the chromitite: blue diamonds: this study; open diamonds: Malitch (2004) and Malitch and Thalhammer (2002)). Data for the clinopyroxenites: dark blue squares: this study; open square: Malitch (2006). Data for placer deposits: open circles: Malitch and Thalhammer (2002), Cabri et al. (1998). (For interpretation of the references to colour in this figure legend, the reader is referred to the web version of this article.)

proposed to define a highly productive single stage process of HSE concentration in clinopyroxenite-dunite complexes.

As an alternative, based on the Pt-Re-Os isotopic data for the Kondyor Pt–Fe alloy grains with variable Os contents (Supplementary Table A2, Fig. 8), Luguet et al. (2019) suggested a different scenario of their evolution. One of Os-poor Pt–Fe alloys with the most unradiogenic composition ($^{187}Os/^{188}Os = 0.110 \pm 0.002$, 1SE) they analyzed was interpreted as reflecting an Archean mantle source, whereas Os isotopic compositions of the majority of Os-rich Pt–Fe alloys with a range of $^{187}Os/^{188}Os$ values between 0.1190 ± 0.0003 and 0.12458 ± 0.00003 were argued to represent variable degrees of mixing/overprinting between the cratonic mantle source and a metasomatizing melt or fluid, likely subduction-related, with radiogenic Os isotopic composition. This scenario, however, is difficult to reconcile with the results of our study for several reasons. First, we obtained Os-isotope data for a Os–Ir alloy, which is represented by a magmatic lamellae that crystallized at high temperatures near-contemporaneously with the host Pt–Fe alloy. Second, the in situ Re-Os-isotope data for the Os-rich alloys from chromitite of our study are identical to the whole-rock Re-Os-isotope data for the host chromitite (Fig. 8). This is difficult to reconcile with the metasomatic scenario of origin for these grains. Third, if Os isotopic compositions of the Os alloys were overprinted by metasomatizing fluids with radiogenic Os isotopic compositions, as suggested by Luguet et al. (2019), this would have yielded a range of positive γOs values, likely similar to those we recorded in Os alloys from zone C clinopyroxenite (i.e., mean $\gamma^{187}Os = +3.44 \pm 0.64$, 2SD, Supplementary Table A2), where they indeed could represent the composition of a metasomatizing fluid with radiogenic Os isotopic composition. This is not observed. Fourth, the most unradiogenic single Pt–Fe alloy grain D-S2 ($^{187}Os/^{188}Os = 0.1101 \pm 0.0025$, 2SD), that was argued by Luguet et al. (2019) to represent the composition of an Archaean component (Fig. 8), has the highest Re/Os value (i.e., $^{187}Re/^{188}Os = 0.0054 \pm 0.0013$, 1SE) compared to those for the rest of the Pt–Fe alloys, which have much higher $^{187}Os/^{188}Os$ values and much lower Re/Os values. This observation is inconsistent with the scenario suggested in Luguet et al. (2019), in which Re/Os values would be expected to increase with the increase in the degree of metasomatic overprinting. We also note that there is no positive correlation (or any correlation, for that matter) between initial $\gamma^{187}Os$ and $\varepsilon^{186}Os$ values in Os-rich Pt–Fe alloys from their study (Supplementary Fig. A1), which would be expected if the metasomatic overprinting did indeed take place.

Taking into account that Os–Ir alloys from our study were formed near-contemporaneously with the Pt–Fe alloys, it is highly unlikely that metasomatizing fluids containing radiogenic Os were physically introduced/incorporated into Os-rich minerals. We consider it more viable that Os-rich alloys were formed prior to Pt–Fe alloys (Fig. 3g-h), or as exsolved phases from primordial Os-bearing Pt–Fe solid solutions, as argued by Malitch and Thalhammer (2002). Based on these lines of evidence, we argue that the Re–Os isotope system within Os–Ir and Pt–Fe alloys at Kondyor remained closed since the time of emplacement of the massif. This is consistent with other studies of Ru-Os-Ir alloys and Ru–Os sulfides (e.g., Badanina et al., 2016; González-Jimenéz et al., 2020; Malitch et al., 2000, 2003, 2013, 2017) that demonstrated high resistance of the Re–Os isotope system within these PGM to post-magmatic events at Witwatersrand (South Africa), Kraubath (Austria), Shetland (Scotland), Finero (Italy), Nurali (Russia) and Andaman (India). The observed Os isotope similarity of primary and secondary PGM assemblages from metamorphosed chromitites from the Shetland dunite-harzburgite massif (Badanina et al., 2016) and the Nurali lherzolite massif, South Urals (Malitch et al., 2016) also supports the conclusion that the secondary PGM have preserved the subchondritic osmium isotope signature of the primary PGM during alteration, showing no evidence for other crustal source contributions (e.g., suprachondritic material) during later thermal events. These Os isotope results are in sharp contrast with the distinctly different Os isotope compositions observed in primary and secondary PGM from the

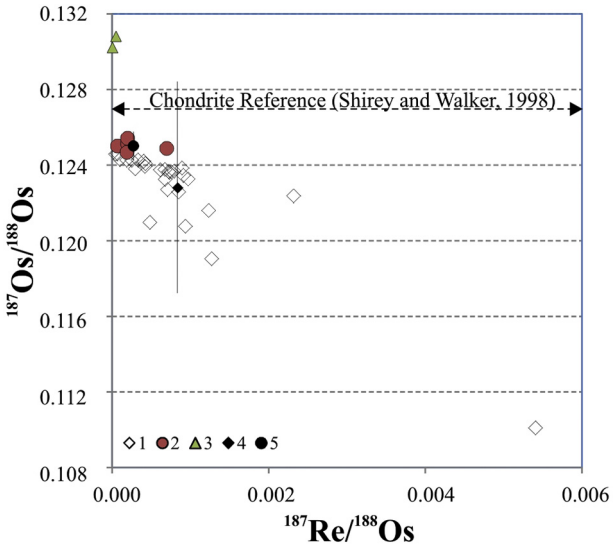

Fig. 8. Variations of $^{187}Os/^{188}Os$ vs. $^{187}Re/^{188}Os$ in chromitite and PGM from chromitite and apatite-phlogopite-magnetite clinopyroxenite (Ap-Phl-Mt Cpx). 1–*in situ* LA MC-ICP-MS analyses of Pt—Fe alloys (after Luguet et al., 2019); 2–*in situ* LA MC-ICP-MS analyses of Os—Ir alloys from chromitite sample K-17, and N-TIMS analysis of chromitite sample K-2014 (zone A, this study), 3–*in situ* LA MC-ICP-MS analyses for Os alloys from Ap-Phl-Mt-Cpx (zone C, this study); 4–black diamond represents a mean value for Pt—Fe alloys ($n = 28$) after Luguet et al. (2019); 5–black circle represents a mean value ($n = 5$) for Os—Ir alloys and chromitite from zone A (this study). Error bars for the $^{187}Os/^{188}Os$ ratio are 2SD (see Supplementary Table A2 for details).

metamorphosed chromitites of the Dobromirtsi ophiolite massif, Bulgaria (González-Jiménez et al., 2012), where the larger range in $^{187}Os/^{188}Os$ within the secondary PGM has been attributed to the interaction of the primary PGM with a metamorphic-hydrothermal fluid, pointing to open-system behavior of the Re–Os system in PGM during metamorphism.

It has been also suggested that dunites of the Kondyor massif have a magmatic origin based on a study of melt inclusions in chromites that indicated that their host chromite likely crystallized from picritic magma (Simonov et al., 2011). In this study, however, we find that the majority of the available data are most consistent with a translithospheric origin for the Kondyor massif proposed by Lazarenkov and Landa (1992) and Burg et al. (2009), which implies that the massif was transferred to the crust in a solid-ductile state, a notion supported by the dome-like structure of surrounding terrigenous rocks and absence of ultramafic dikes (excluding a stockwork zone C in the southeastern part of the massif), which would have been abundant in case the Kondyor massif had originated from picritic or lamproitic magmas, crystallized at the supracrustal levels. PGE-bearing ultramafic massifs, such as Kondyor, are unequivocally connected with deep levels of tectonosphere (Malitch, 1999). In this sense they are comparable to 250 Ma PGE-Cu-Ni-bearing Noril'sk-type ultramafic-mafic intrusions, which are closely related to rift structures (Tuganova, 2000).

In contrast to the PGM from the zone A chromitites with chondritic initial $^{187}Os/^{188}Os$ composition, the Os-rich alloys from the clinopyroxenites within the stockwork-like zone C at Kondyor show high initial $\gamma^{187}Os$ values ranging between +3.2 and + 3.7, Fig. 7, Table 4). This indicates that the source of the zone C clinopyroxenites evolved with a long-term suprachondritic Re/Os ratio. This enrichment in Re could be the result of reaction of the highly Re-enriched lamproitic melts with the wall-rock dunites during formation of the zone C stockwork clinopyroxenite complex, a scenario proposed by Burg et al. (2009) to explain the origin of the clinopyroxenite complex rocks.

We further propose that the suprachondritic initial $^{187}Os/^{188}Os$ values that have been detected in detrital Os-rich grains (Cabri et al., 1998; this study, Fig. 7) may also indicate derivation of these PGM

from a rock lithology other than chromitite. As is evident from the Os-rich alloy grains from the zone C clinopyroxenites at Kondyor, the latter can be considered as one of the lithological sources of the PGM in placers. The Os isotopic evidence supports a distinct origin for the dunites/chromitites and the stockwork clinopyroxenites, proposed on the basis of geological, geochemical, and mineralogical data (Avdontsev and Malich, 1987; Avdontsev and Malitch, 1989; Efimov et al., 2012; Gurovitch et al., 1994; Luguet et al., 2019; Malitch, 1999; Malitch et al., 2012). We, thus, propose that Os isotope data obtained from samples with well-constrained geological position (e.g., PGM, chromitite, clinopyroxenite, etc.) can provide important information bearing on their HSE sources. Conclusions based only on Os isotope data for detrital Os-rich alloy grains or deduced from a limited number of Os-isotope analyses must be treated with caution.

7. Conclusions

1. A multi-technique approach, including a specific separation technique to concentrate PGM, and the use of in-situ analytical techniques for geochemical and isotopic analysis provided a new set of mineralogical and isotope-geochemical constraints on the origin of accessory PGM from the core-zone A dunite and stockwork-type zone C clinopyroxenite of the Kondyor zoned-type massif.
2. The "M-shaped" BSE-normalized HSE patterns with positive peaks at Pt and Ir are characteristic of the zone A chromitites; this pattern is similar to that of chromitites from the Uralian-Alaskan type complexes. In contrast, the zone C clinopyroxenite assemblage shows enrichments in Pt and Pd, resulting in a positively sloped BSE-normalized HSE pattern, similar to that of mantle- derived melts.
3. The presence of Ir-rich Pt–Fe alloys in the zone A chromitites and Pd-rich Pt–Fe alloys in the zone C clinopyroxenites of the Kondyor massif is considered to be a diagnostic feature of zoned-type ultramafic complexes. We propose that such mineralogical characteristics may help distinguish between the specific source rocks for the particular Pt–Fe type of mineralization in cases where the host rock is unknown.
4. The Re–Os isotope results for the zone A samples identify a limited range of $\gamma^{187}Os_{(T=250\ Ma)}$ values for Os-rich alloy grains (between −0.4 and + 0.1), which is similar to that of chromitites (from −0.5 to +0.3). These $\gamma^{187}Os_{(T=250\ Ma)}$ values are indicative of a common source for the HSE that evolved with near-chondritic Re/Os. These data also imply that the osmium budget of chromitites and the host dunites was largely controlled by the Os-rich alloys. We further conclude that there was a single event of PGE concentration and PGM formation within the core-zone A dunite.
5. The Re-Os-isotope data for the Os alloy grains from the zone C clinopyroxenites ($\gamma^{187}Os_{(T=125\ Ma)}$ values range from +3.2 to +3.7) indicate derivation from the source that evolved with long-term suprachondritic Re/Os ratio. This long-term enrichment in Re could be the result of reaction of the highly Re-enriched lamproitic melts with the wall-rock dunites during formation of the zone C stockwork clinopyroxenite complex. The similarly suprachondritic initial $\gamma^{187}Os_{(T)}$ values, which have been also detected in the detrital Os-bearing PGM from the spatially associated placer deposit (Cabri et al., 1998; Malitch, 2006), provide evidence that these detrital PGM were likely derived from the zone C clinopyroxenites of the Kondyor massif.
6. The mineralogical, geochemical, and Os isotope data are consistent with a high-temperature origin of the studied PGM and imply distinct HSE sources of the HSE mineralization in the ultramafic rocks of the Kondyor massif.

Supplementary data to this article can be found online at https://doi.org/10.1016/j.lithos.2020.105800.

Declaration of Competing Interest

The authors declare that they have no known competing financial interests or personal relationships that could have appeared to influence the work reported in this paper.

Acknowledgements

This study was supported by Ministry of Science and Higher Education of the Russian Federation (state assignment # AAAA-A18-118052590026-5), Russian Foundation for Basic Research grant 16-05-00967-a to KNM, Australian Research Council grant FT110100685 to EAB, and by NSF Petrology and Geochemistry - National Science Foundation Petrology and Geochemistry (USA) grant EAR 1754186 to ISP. The analytical work at CCFS/GEMOC was funded by DEST Systemic Infrastructure - Department of Education, Science and Training Systemic Infrastructure (Australia) Grants, ARC LIEF, NCRIS, industry partners, and Macquarie University. We thank Vladimir Knauf, Thomas Meisel, and Vera Khiller for help and advice, Ambre Luguet and an anonymous reviewer for critical comments, and Guest Editor Jose-Maria González-Jimenéz and Co-Editor-in-Chief Greg Shellnut for useful suggestions and editorial handling of the manuscript. This is contribution 1523 from the ARC Centre of Excellence for Core to Crust Fluid Systems (http://www.ccfs.mq.edu.au) and 1400 in the GEMOC Key Centre (http://www.gemoc.mq.edu.au).

References

Auge´, T., Legendre, O., 1992. Pt–Fe nuggets from alluvial deposits in eastern Madagascar. Can. Mineral. 30, 983–1004.
Amosse´, J., Dable´, P., Allibert, M., 2000. Thermochemical behaviour of Pt, Ir, Rh, and Ru vs fO_2 and fS_2 in a basaltic melt. Implications for the differentiation and precipitation of these elements. Mineral. Petrol. 68, 29–62.
Auge´, T., Genna, A., Legendre, O., Ivanov, K.S., Volchenko, Y.A., 2005. Primary platinum mineralization in the Nizhny Tagil and Kachkanar ultramafic complexes, Urals, Russia: a genetic model for PGE concentration in chromite-rich zones. Econ. Geol. 100, 707–732.
Andreev, G.V., 1987. The Kondyor Massif of Ultramafic and Alkaline Rocks. Nauka, Novosibirsk, Russia, p. 75 (in Russian).
Andrews, D.R.A., Brenan, J.M., 2002. Phase-equilibrium constraints on the magmatic origin of laurite + Ru-Os-Ir alloy. Can. Mineral. 40, 1721–1735.
Avdontsev, S.N., Malich, K.N., 1987. Physicochemical conditions of iron-titanium oxide formation in rocks of the Kondyor alkalic ultramafic pluton. Trans. (Dokl.) USSR Acad. Sci./Earth Sci. Sect. 296 (5), 225–227.
Avdontsev, S.N., Malitch, K.N., 1989. Geodynamic model of formation of massifs of the Kondyor complex. Sov. Geol. Geophys. 30, 23–27.
Badanina, I.Y., Malitch, K.N., Lord, R.A., Meisel, T.C., 2013a. Origin of primary PGM assemblage in chromitite from a mantle tectonite at Harold's Grave (Shetland ophiolite complex, Scotland). Mineral. Petrol. 107, 963–970.
Badanina, I.Yu., Malitch, K.N., Murzin, V.V., Khiller, V.V., Glavatskikh, S.P., 2013b. Mineralogical and geochemical characteristics of PGE mineralization of the Verkh-Neivinsk dunite-harzburgite massif (Middle Urals, Russia). Proc. Inst. Geol. Geochem. UB RAS 160, 188–192 (in Russian).
Badanina, I.Yu., Malitch, K.N., Lord, R.A., Belousova, E.A., Meisel, T.C., 2016. Closed-system behaviour of the Re-Os isotope system recorded in primary and secondary PGM assemblages: evidence from a mantle chromitite at Harold's Grave (Shetland ophiolite Complex, Scotland). Ore Geol. Rev. 75, 174–185. https://doi.org/10.1016/j.oregeorev.2015.12.014.
Barkov, A.Y., Cabri, L.J., 2019. Variations of major and minor elements in Pt–Fe alloy minerals: a review and new observations. Minerals 9, 25. https://doi.org/10.3390/min9010025.
Barkov, A.Y., Shvedov, G.I., Polonyankin, A.A., Martin, R.F., 2017. New and unusual Pd-Tl-bearing mineralization in the Anomal'nyi deposit, Kondyor concentrically zoned complex, northern Khabarovskiy kray, Russia. Mineral. Mag. 81 (3), 679–688.
Becker, H., Horan, M.F., Walker, R.J., Gao, S., Lorand, J.-P., Rudnick, R.L., 2006. Highly siderophile element compositionof the Earth's primitive upper mantle: constraints from new data on peridotite massifs and xenoliths. Geochim. Cosmochim. Acta 70 (17), 4528–4550.
Birck, J.-L., Roy-Barman, M., Capmas, F., 1997. Re–Os Isotopic Measurements at Femtomole Level in Natural Samples. 20. Geostandards Newsletter, pp. 19–27.
Brenan, J.M., Andrews, D., 2001. High-temperature stability of laurite and Ru-Os-Ir alloy and their role in PGE fractionation in mafic magmas. Can. Mineral. 39, 341–360.
Burg, J.P., Bodinier, J.-L., Gerya, N., Bedini, R.-M., Boudier, F., Dautria, J.-M., Prikhodko, V., Efimov, A., Pupier, E., Balanec, J.-L., 2009. Translithospheric mantle diapirism: geological evidence and numerical modeling of the Kondyor zoned ultramafic complex (Russian Far-East). J. Petrol. 50 (2), 289–321.
Cabri, L.J., Laflamme, J.H.G., 1997. Platinum-group minerals from the Konder massif, Russian Far East. Mineral. Rec. 28, 97–106.

Cabri, L.J., Stern, R.A., Czamanske, G.K., 1998. Osmium isotope measurements of the Pt-Fe alloy placer nuggets from the Konder Intrusion using a Shrimp II Ion Microprobe. 8th International Platinum Symposium Abstracts, pp. 55–58.

Cohen, A.S., Waters, F.G., 1996. Separation of osmium from geological materials by solvent extraction for analysis by thermal ionisation mass spectrometry. Anal. Chim. Acta 332 (2–3), 269–275.

Creaser, R.A., Papanastassiou, D.A., Wasserburg, G.J., 1991. Negative thermal ion mass spectrometry of osmium, rhenium, and iridium. Geochim. Cosmochim. Acta 55, 397–401.

Efimov, A.A., 1984. Gabbro-Ultrabasic Complexes of the Urals and a Problem of Ophiolites. Nauka, Moscow 232 p. (in Russian).

Efimov, A.A., Tavrin, I.F., 1978. Common origin of platinum-bearing dunites of the Urals and Aldan Shield. Dokl. Acad. Sci. USSR 243, 75–77.

Efimov, A.A., Ronkin, Yu.L., Malich, K.N., Lepikhina, G.A., 2012. New Sm-Nd and Rb-Sr (ID-TIMS) isotope data for apatite-phlogopite clinopyroxenites from the dunite "core" of the Konder Massif, Aldan Shield. Dokl. Earth Sci. 445, 956–961.

El'yanov, A.A., Andreev, G.V., 1991. Magmatism and Metallogeny of Platform Areas Affected by Multistage Activization. Nauka Press, Novosibirsk 168 p. (in Russian).

El'yanov, A.A., Moralev, V.M., 1961. New data on age of ultrabasic and alkaline rocks of the Aldan Shield. Dokl. Acad. Sci. USSR 141, 1163–1165.

Evstigneeva, T.L., 2009. Phases in Pt-Fe system. Electron. Sci. Inform. J. 1 (27) "Vestnik Otdelenia nauk o Zemle RAN". http://www.scgis.ru/russian/cp1251/h_dgggms/1-2009/informbul-1_2009/mineral-6e.pdf.

Fonseca, R.O.C., Brückel, K., Bragagni, A., Leitzke, F.P., Speelmanns, I.M., Wainwright, A.N., 2017. Fractionation of rhenium from osmium during noble metal alloy formation in association with sulfides: implications for the interpretation of model ages in alloy-bearing magmatic rocks. Geochim. Cosmochim. Acta 216, 184–200.

Garuti, G., Pushkarev, E.V., Zaccarini, F., 2002. Composition and paragenesis of Pt alloys from chromitites of the Uralian-Alaskan-type Kytlym and Uktus complexes, Northern and Central Urals, Russia. Can. Mineral. 40, 1127–1146.

González-Jiménez, J.M., Gervilla, F., Proenza, J.A., Kerestedjian, T., Augé, T., Bailly, L., 2009. Zoning of laurite (RuS_2)-erlichmanite (OsS_2): implications for the genesis of PGM in ophiolite chromitites. Eur. J. Mineral. 21, 419–432.

González-Jiménez, J.M., Griffin, W.L., Gervilla, F., Kerestedjian, T.N., O'Reilly, S.Y., Proenza, J.A., Pearson, N.J., Sergeeva, I., 2012. Metamorphism disturbs the Re-Os signatures of platinum-group minerals in ophiolite chromitites. Geology 40, 659–662.

González-Jimenéz, J.M., Locmelis, M., Belousova, E., Griffin, W., Gervilla, F., Kerestedjian, T.N., O'Reilly, S.Y., Pearson, N.J., Sergeeva, I., 2015. Genesis and tectonic implications of podiform chromitites in the metamorphosed ultramafic massif of Dobromirtsi (Bulgaria). Gondwana Res. 27, 555–574.

González-Jimenéz, J.M., Mondal, S.K., Ghosh, B., Griffin, W.L., O'Reilly, S.Y., 2020. Re-Os isotope systematics of sulfides in chromitites and host lherzolites of the Andaman ophiolite, India. Minerals 10, 686. https://doi.org/10.3390/min10080686.

Guillou-Frottier, L., Burov, E., Augé, T., Gloaguen, E., 2014. Reological conditions for emplacement of Ural-Alaskan-type ultramafic complexes. Tectonophysics 631, 130–145.

Gurovitch, V.G., Zemlyanukhin, V.N., Emel'yanenko, E.P., Karetnikov, A.S., Kvasov, A.I., Lazarenkov, V.G., Malitch, K.N., Mochalov, A.G., Prikhod'ko, V.S., Stepashko, A.A., 1994. Geology, Petrology and Ore-Forming Potential of the Kondyor Massif. Nauka Press, Moscow, Russia, p. 176 (in Russian).

Harris, D.C., Cabri, L.J., 1991. Nomenclature of platinum-group-element alloys: review and revision. Can. Mineral. 29, 231–237.

Johan, Z., 2002. Alaskan-type complexes and their platinum-group element mineralization. In: Cabri, L.J. (Ed.), The Geology, Geochemistry, Mineralogy and Mineral Beneficiation of Platinum-Group Elements. Special Volume, 54. Canadian Institute of Mining and Metallurgy, pp. 299–319.

Johan, Z., Slansky, E., Barron, L.M., Suppel, D., 1989. Platinum mineralization in the Alaskan-type intrusive complexes near Fifield, New South Wales, Australia. I. Platinum-group minerals in clinopyroxenites of the Kelvin Grove prospect, Owendale intrusion. Mineral. Petrol. 40, 289–309.

Kloprogge, J.T., Wood, B.J., 2018. X-ray photoelectron spectroscopy and raman microscopy of a ferroan platinum crystal from the Kondyor massif, Russian Far East. Spectrosc. Lett. 52 (1), 43–48.

Korotkov, V.A., Kuznetsov, A.P., Leikin, A.Yu., Velikaya, T.I., 2016. Mass spectrometric determination of Pt, Pd, Rh, Ru, Ir, Os, Au and Ag with preliminary collecting on nickel matte without matrix resetting. Abstracts of the XXI International Chernyaev Conference on Chemistry, Analysis and Technology of Platinum Metals. Institute of Inorganic Chemistry SB RAS Press, Novosibirsk, p. 129.

Lazarenkov, V.G., Landa, E.A., 1992. Evidences for non-intrusive nature of the Kondyor massif and problems of the mantle diapirism. Proc. Russ. Acad. Sci. Geol. Ser. 6, 102–113 (in Russin).

Lazarenkov, V.G., Malitch, K.N., Sah'yanov, L.O., 1992. PGE-Mineralization of Zoned Ultrabasic and Komatiitic Massifs. Russia, Nedra Press, St. Petersburg, p. 217 (in Russian).

Lorand, J.-P., Alard, O., 2001. Platinum-group element abundances in the upper mantle: new constraints from in situ and whole-rock analyses of Massif Central xenoliths (France). Geochim. Cosmochim. Acta 65, 2789–2806.

Luguet, A., Nowell, G.M., Pushkarev, E., Ballhaus, C., Wirth, R., Schreiber, A., Gottman, I., 2019. ^{190}Pt-^{186}Os geochronometer reveals open system behaviour of ^{190}Pt-^{4}He isotope system. Geochem. Perspect. Lett. 11, 44–48.

Malitch, K.N., 1998. Peculiarities of platinum-group elements distribution in ultramafites of clinopyroxenite–dunite massives as an indicator of their origin. In: Laverov, N.P., Distler, V.V. (Eds.), International Platinum. St. Petersburg-Athens, Theophrastus Publications, pp. 129–140.

Malitch, K.N., 1999. Platinum-Group Elements in Clinopyroxenite-Dunite Massifs of the Eastern Siberia (Geochemistry, Mineralogy, and Genesis). Saint Petersburg Cartographic Factory VSEGEI Press, St. Petersburg, p. 296 (in Russian).

Malitch, K.N., 2004. Morphology, chemical composition and osmium-isotope systematics of osmium minerals from the Guli massif (Maymecha-Kotuy province, Siberian platform). Nat. Resour. Taimyr 2, 258–276 (in Russian).

Malitch, K.N., 2006. Os isotope systematics of Os-rich alloys and sulfides from continental and oceanic mantle: new data. Geochim. Cosmochim. Acta 70 (18S), A386.

Malitch, K.N., Thalhammer, O.A.R., 2002. Pt-Fe nuggets derived from clinopyroxenite-dunite massifs, Russia: a structural, compositional and osmium-isotope study. Can. Mineral. 40, 395–418.

Malitch, K.N., Badanina, I.Yu., 2015. Iron-platinum alloys from chromitites of the Nizhny Tagil and Kondyor clinopyroxenite–dunite massifs (Russia). Dokl. Earth Sci. 462 (2), 634–637.

Malitch, K.N., Kostoyanov, A.I., Merkle, R.K.W., 2000. Mineral composition and osmium isotopes of PGE-mineralization from the Eastern Witwatersrand, South Africa. Geol. Ore Depos. 42 (3), 253–266.

Malitch, K.N., Melcher, F., Mühlhans, H., 2001. Palladium and gold mineralization in podiform chromitite at Kraubath, Austria. Mineral. Petrol. 73, 247–277.

Malitch, K.N., Auge, T., Badanina, I.Yu., Goncharov, M.M., Junk, S.A., Pernicka, E., 2002. Os-rich nuggets from Au-PGE placers of the Maimecha-Kotui Province, Russia: a multidisciplinary study. Mineral. Petrol. 76, 121–148.

Malitch, K.N., Junk, S.A., Thalhammer, O.A.R., Melcher, F., Knauf, V.V., Pernicka, E., Stumpfl, E.F., 2003. Laurite and ruarsite from podiform chromitites at Kraubath and Hochgrцssen, Austria: new insights from osmium isotopes. Can. Mineral. 41, 331–352.

Malitch, K.N., Efimov, A.A., Badanina, I.Yu., 2012. The age of Kondyor massif dunites (Aldan Province, Russia): first U-Pb isotopic data. Dokl. Earth Sci. 446 (1), 1054–1058.

Malitch, K.N., Badanina, I.Yu., Knauf, V.V., Meisel, T., 2013. Platinum-group element geochemistry and mineralogy of dunite-harzburgite and clinopyroxenite-dunite massifs. Proc. Inst. Geol. Geochem. UB RAS 160, 255–260 (in Russian).

Malitch, K.N., Belousova, E.A., Griffin, W.L., Badanina, I.Yu., Knauf, V.V., O'Reilly, S.Y., Pearson, N.J., 2017. Laurite and zircon from the Finero chromitites (Italy): new insights into evolution of the subcontinental mantle. Ore Geol. Rev. 90, 210–225.

Malitch, K.N., Anikina, E.V., Badanina, I.Yu., Belousova, E.A., Pushkarev, E.V., Khiller, V.V., 2016. Chemical composition and osmium isotope systematics of primary and secondary platinum-group mineral assemblages from high-Mg chromitite of the Nurali lherzolite massif, South Urals, Russia. Geol. Ore Depos. 58 (1), 1–19.

Meisel, T., Moser, J., Fellner, N., Wegscheider, W., Schoenberg, R., 2001. Simplified method for the determination of Ru, Pd, Re, Os, Ir and Pt in chromitites and other geological materials by isotope dilution ICPMS and acid digestion. Analyst 126, 322–328.

Meisel, T., Fellner, N., Moser, J., 2003. A simple procedure for the determination of platinum-group elements and rhenium (Ru, Ph, Pd, Re, Os, Ir and Pt) using ID-ICPMS with an inexpensive on-line- matrix separation in geological and environmental materials. J. Anal. At. Spectrom. 18, 720–726.

Merkle, R.K.W., Malitch, K.N., Grasser, P.P.H., Badanina, I.Yu., 2012. Native osmium from the Guli Massif, Northern Siberia (Russia). Mineral. Petrol. 104, 115–127.

Mochalov, A.G., Khoroshilova, T.S., 1998. The Konder alluvial placer of platinum metals. In: Laverov, N.P., Distler, V.V. (Eds.), International Platinum. St. Petersburg-Athens, Theophrastus Publications, pp. 206–220.

Mochalov, A.G., Yakubovich, O.V., Bortnikov, N.S., 2016. ^{190}Pt- ^{4}He age of PGE ores in the alkaline-ultramafic Kondyor Massif (Khabarovsk District, Russia). Dokl. Earth Sci. 469, 846–850.

Nekrasov, I.Ya., Lennikov, A.M., Oktyabr'skiy, R.A., Zalishchak, B.L., Sapin, V.I., 1994. Petrology and Platinum Potential of the Ring Alkaline-Ultramafic Complexes. Nauka Press, Moscow 381 p. (in Russian).

Nixon, G.T., Cabri, L.J., Laflamme, G.J.H., 1990. Platinum group-element mineralization in lode and placer deposits associated with the Tulameen Alaskan-type complex, British Columbia. Can. Mineral. 28, 503–535.

Nowell, G.M., Pearson, D.G., Parman, S.W., Luguet, A., Hanski, E., 2008. Precise and accurate $^{186}Os/^{188}Os$ and $^{187}Os/^{188}Os$ measurements by multi-collector plasma ionisation mass spectrometry, part II: laser ablation and its application to single-grain Pt-Os and Re-Os geochronology. Chem. Geol. 248, 394–426.

Okrugin, A.V., 2011. Origin of platinum-group minerals in mafic-ultramafic rocks: from dispersed elements to nuggets. Can. Mineral. 49, 1397–1412.

Orlova, M.P., 1992. Geology and genesis of the Konder massif. Geol. Pac. Ocean 8, 120–132.

Orlova, M.P., Avdeeva, O.I., Fyodorova, I.V., Yakovleva, L.V., 1978. New data about radiological dating of the Kondyor massif and enclosing rocks (eastern part of the Aldan Shield). Dokl. Akad. Nauk 240 (3), 677–680 (in Russian).

Paliulionyte, V., Meisel, T., Ramminger, P., Kettisch, P., 2006. High pressure asher digestion and an isotope dilution-ICP-MS method for the determination of platinum-group element concentrations in chromitite reference materials CHR-Bkg, GAN Pt-1 and HHH. Geostand. Geoanal. Res. 30, 87–96.

Pearson, N.J., Alard, O., Griffin, W.L., Jackson, S.E., O'Reilly, S.Y., 2002. In situ measurement of Re-Os isotopes in mantle sulfides by laser ablation multicollector-inductively coupled plasma mass spectrometry: analytical methods and preliminary results. Geochim. Cosmochim. Acta 66, 1037–1050.

Puchtel, I.S., Touboul, M., Blichert-Toft, J., Walker, R.J., Brandon, A.D., Nicklas, R.W., Kulikov, V.S., Samsonov, A.V., 2016. Lithophile and siderophile element systematics of the mantle at the Archean-Proterozoic boundary: evidence from 2.4 Ga komatiites. Geochim. Cosmochim. Acta 180, 227–255.

Puchtel, I.S., Blichert-Toft, J., Touboul, M., Walker, R.J., 2018. ^{182}W and HSE constraints from 2.7 Ga komatiites on the heterogeneous nature of the Archean mantle. Geochim. Cosmochim. Acta 228, 1–26.

Puchtel, I.S., Mundl-Petermeier, A., Horan, M., Hanski, E.J., Blichert-Toft, J., Walker, R.J., 2020. Ultra-depleted 2.05 Ga komatiites of Finnish Lapland: products of grainy late accretion or core-mantle interaction? Chem. Geol. 554, 119801.

Pushkarev, E.V., Kamenetsky, V.S., Morozova, A.V., Khiller, V.V., Glavatskykh, S.P., Rodemann, T., 2015. Ontogeny of Ore Cr-spinel and composition of inclusions as indicators of the pneumatolytic-hydrothermal origin of PGM-bearing chromitites from Kondyor massif, the Aldan Shield. Geol. Ore Depos. 57, 352–380.

Pushkaryov, Yu.D., Kostoyanov, A.I., Orlova, M.P., Bogomolov, E.S., 2002. Peculiarities of Rb-Sr, Sm-Nd, Pb-Pb,Re-Os and K-Ar isotope systems in the Kondyor massif: mantle susbstratum, enriched in PGE. Reg. Geol. Metall. 16, 80–91 (in Russian).

Rehkämper, M., Halliday, A.N., 1997. Development and application of new ion-exchange techniques for the separation of the platinum-group and other siderophile elements from geological samples. Talanta 44 (4), 663–672.

Rozhkov, I.S., Kitsul, V.I., Razin, L.V., Borishanskaya, S.S., 1962. Platinum of Aldan Shield. Academy of Sciences of the USSR Press, Moscow, Russia, p. 280 (in Russian).

Rudashevsky, N.S., 1989. Platinum-Group Elements in Rocks of Ultramafic Formations (Mineralogy and Genesis). Habil. Thesis. Mining Institute, Leningrad, Russia (in Russian).

Rudashevsky, N.S., Burakov, B.E., Malitch, K.N., Khaetskiy, V.V., 1992. Accessory platinum mineralization of chromitites from the Kondyor ultramafic Massif. Mineral. Zhurnal. 14 (5), 12–22 (in Russian).

Rudashevsky, N.S., Fomenko, A.S., Malitch, K.N., 1994. Primary PGE mineralization of dunites and clinopyroxenites of the Kondyor intrusion (Aldan Shield). VII Platinum International Symposium Abstracts. Moskovsky Kontakt Press, Moscow, p. 102.

Shcheka, G.G., Lehmann, B., Gierth, E., Gömann, K., Wallianos, A., 2004. Macrocrystals of Pt–Fe alloy from the Kondyor PGE placer deposit, Khabarovskiy Kray, Russia: trace-element content, mineral inclusions and reaction assemblages. Can. Mineral. 42, 601–617.

Shirey, S.B., Walker, R.J., 1998. The Re–Os isotope system in cosmochemistry and high temperature geochemistry. Annu. Rev. Earth Planet. Sci. 26, 423–500.

Shnai, G.K., Kuranova, V.N., 1981. New evidence for age of dunite in composite massifs of ultramafic-alkaline composition. Dokl. Akad. Nauk SSSR 261, 950–952 (in Russian).

Shukolyukov, Yu.A., Yakubovich, O.V., Mochalov, A.G., Kotov, A.B., Sal'nikova, E.B., Yakovleva, S.Z., Korneev, S.I., Gorokhovskii, B.M., 2012. New geochronometer for the direct isotopic dating of native platinum minerals (^{190}Pt-^{4}He method). Petrology 20, 491–507.

Simonov, V.A., Prikhod'ko, V.S., Kovyazin, S.V., 2011. Genesis of platiniferous massifs in the southeastern Siberian Platform. Petrology 19, 549–567.

Smoliar, M.I., Walker, R.J., Morgan, J.W., 1996. Re-Os ages of group IIA, IIIA, IVA, and IVB meteorites. Science 271, 1099–1102.

Sushkin, L.B., 1996. Characteristic features of native elements at the Kondyor deposit. Geol. Pac. Ocean 12, 915–924.

Tessalina, S.G., Malitch, K.N., Augé, T., Puchkov, V.N., Belousova, E., McInnes, B.I.A., 2015. Origin of the Nizhny Tagil clinopyroxenite-dunite massif (uralian platinum belt, Russia): insights from PGE and Os isotope systematics. J. Petrol. 56, 2297–2318.

Tolstykh, N.D., Sidorov, E.G., Krivenko, A.P., 2005. Platinum-group element placers associated with Ural-Alaskan type complexes. Mineral. Assoc. Can. Short Course 35, 113–143.

Tuganova, E.V., 2000. Petrographic Types, Genesis and Regularities of Distribution of Ni-Cu-PGE Sulfide Deposits. VSEGEI Press, St.-Petersburg, p. 102 (in Russian).

Walker, R.J., Carlson, R.W., Shirey, S.B., Boyd, F.R., 1989. Os, Sr, Nd, and Pb isotope systematics of Southern African peridotite xenoliths: implications for the chemical evolution of subcontinental mantle. Geochim. Cosmochim. Acta 53, 1583–1595.

Zaccarini, F., Garuti, G., Pushkarev, E., Thalhammer, O., 2018. Origin of platinum-group minerals (PGM) inclusions in chromite deposits of the Urals. Minerals 8, 379. https://doi.org/10.3390/min8090379.

Zemlyanukhin, V.N., Prikhodko, V.S., 1997. Structures and petrotextures of the ultrabasic cores of ring massifs in the Russian Far East. Geol. Pac. Ocean 13, 689–700.

Zientek, M., Padriarto, B., Simandjuntak, H.R.W., Wikrama, A., Oscarson, R.L., Meier, A.L., Carlson, R.R., 1992. Placer and lode platinum group minerals in South Kalimantan, Indonesia: evidence for derivation from Alaskan-type ultramafic intrusions. Aust. J. Earth Sci. 39, 405–417.